Supporting Information

Strong Single- and Two-Photon Luminescence Enhancement by Non-Radiative Energy Transfer across Layered Heterostructure

Medha Dandu, Rabindra Biswas, Sarthak Das, Sangeeth Kallatt, Suman Chatterjee, Mehak Mahajan, Varun Raghunathan, Kausik Majumdar*

Department of Electrical Communication Engineering, Indian Institute of Science, Bangalore 560012, India

*Corresponding author, email: *kausikm@iisc.ac.in*

Different layered heterostructures used for PL measurements and Raman characterization

Figure S1a shows the optical image of the 1L-MoS_2/$SnSe_2$ junction (sample J1) used for PL spectroscopy and mapping. 1L-MoS_2 is characterized with Raman spectroscopy with 532 nm for A_{1g} and E_{2g}^1 modes which were obtained at 404.8 cm^{-1} and 385.1 cm^{-1} respectively.[1] Raman shift at the $SnSe_2$ region shows its E_g and A_{1g} peaks at 110.6 cm^{-1} and 184.8 cm^{-1} respectively. On the junction region, A_{1g} and E_{2g}^1 modes of 1L-MoS_2 are quenched completely as shown in Figure S1b. Figure S1c and S1d show the optical images of 1L-MoS_2/TaS_2 and 1L-WS_2/$SnSe_2$ junctions used for PL characterization in this work.

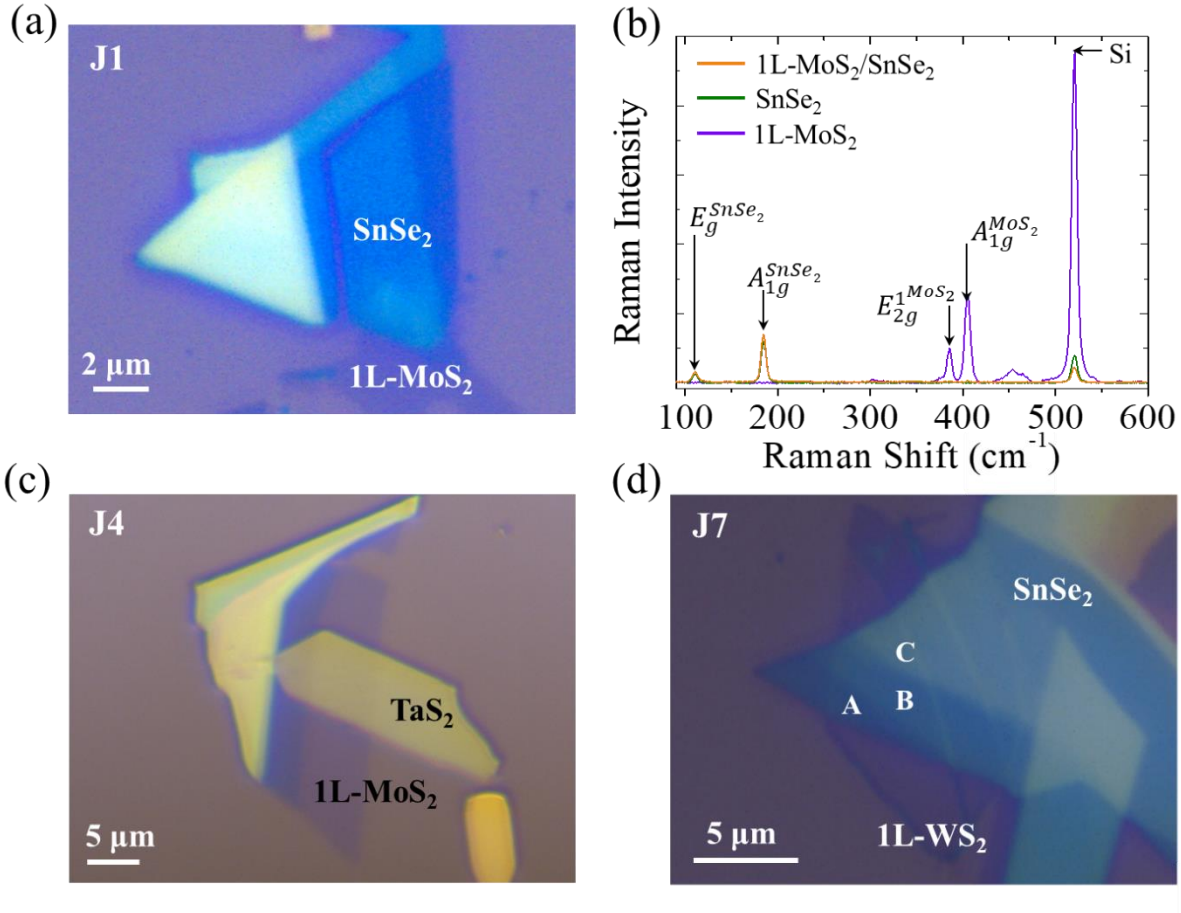

Figure S1: (a) Optical image of the 1L-MoS_2/$SnSe_2$ junction (J1) described in Figure 1a. (b) Raman shift of 1L-MoS_2, $SnSe_2$ and the junction from sample J1 characterized with 532 nm laser. (c) Optical image of the 1L-MoS_2/TaS_2 junction J4 whose spectra are represented in Figure 1f. (d) Optical image of the 1L-WS_2/$SnSe_2$ junction J7 described in figure 2e-f.

PL enhancement across 1L-MoS_2/$SnSe_2$ from multiple samples (J2 and J3)

PL enhancement of 1L-MoS_2 on 1L-MoS_2/$SnSe_2$ junction is verified across other samples J2 and J3 with both 633 nm and 532 nm excitation.

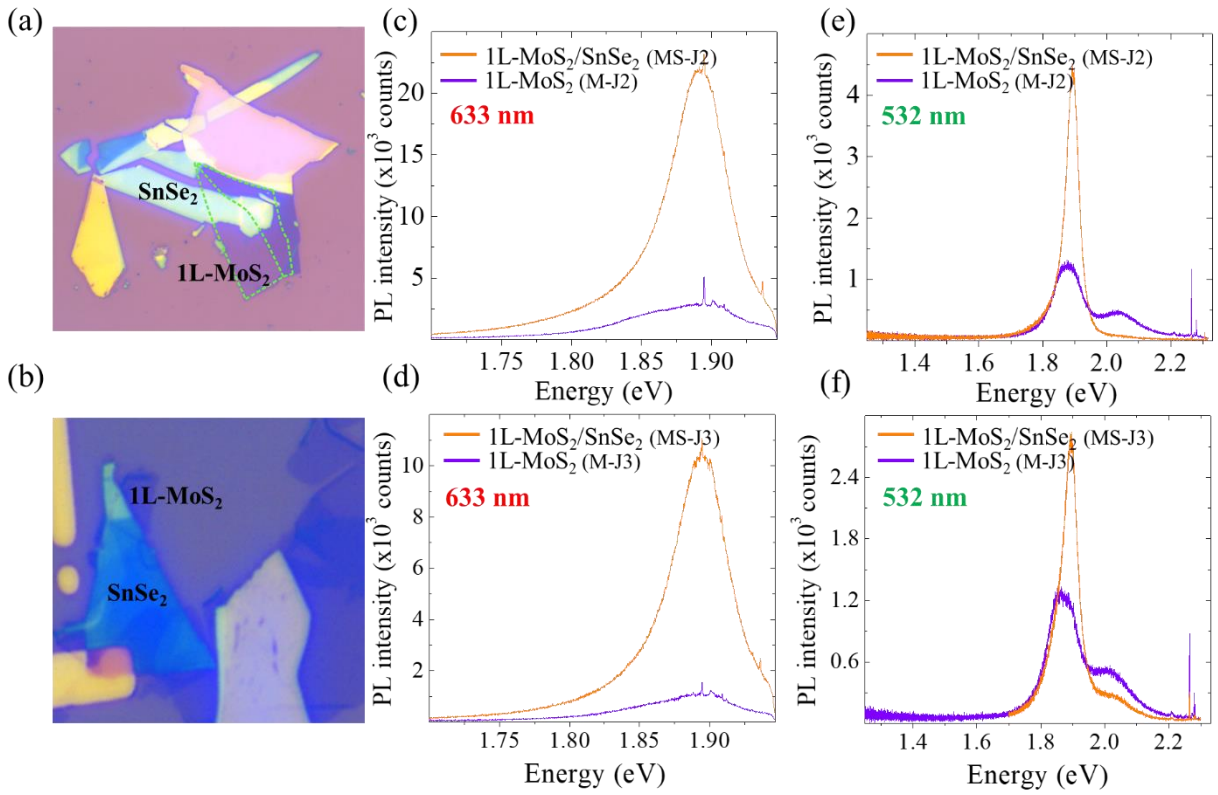

Figure S2: (a-b) The optical images of 1L-MoS_2/$SnSe_2$ junctions from samples J2 and J3. Sample J2 is used to characterize temperature dependence of PL enhancement. (c-d) 633 nm PL spectra of isolated 1L-MoS_2 (violet) and junction (orange) regions. (e-f) 532 nm PL spectra of isolated 1L-MoS_2 (violet) and junction (orange) regions.

Photoluminescence spectroscopy across another 1L-MoS_2/hBN/$SnSe_2$ sample (J6)

Due to the manifestation of efficient FRET across 1L-MoS_2/$SnSe_2$, PL enhancement persists even with insertion of spacer layer, hBN as discussed in the main text from sample J5. We verify this PL enhancement with both 633 nm and 532 nm across 1L-MoS_2/hBN/$SnSe_2$ with another sample J6.

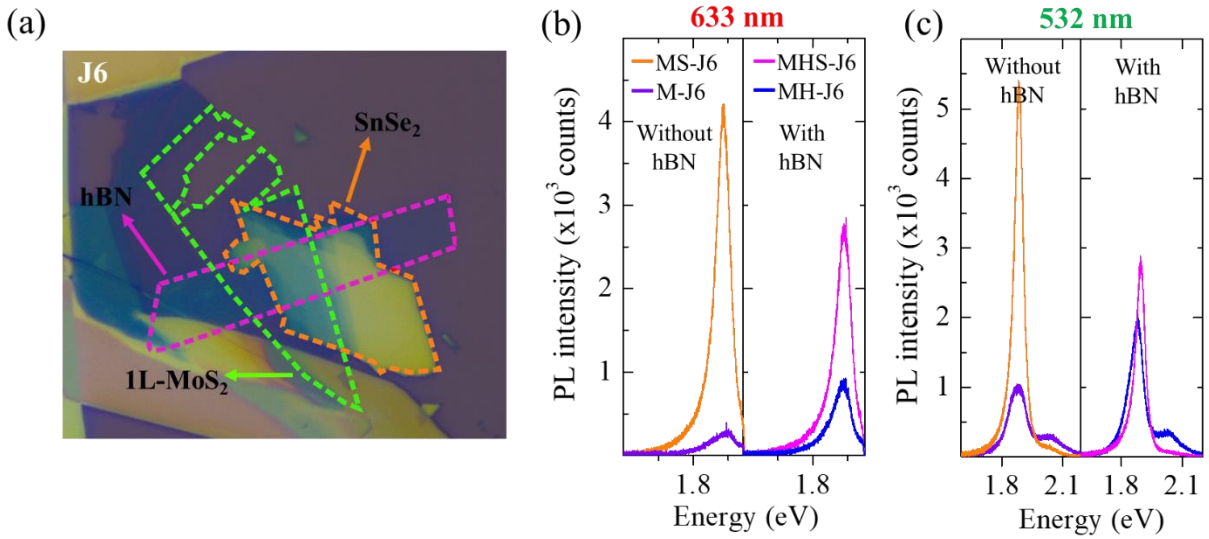

Figure S3: (a) Optical image of sample J6 used to verify PL enhancement of 1L-MoS_2 on the 1L-MoS_2/hBN/$SnSe_2$ junction. (b-c) 633 nm and 532 nm PL spectra of 1L-MoS_2/$SnSe_2$ junction and the corresponding isolated 1L-MoS_2 control without (left panel) and with the presence of hBN (right panel) in the sample J6.

Reflectance contrast of $SnSe_2$ at low temperature

Reflectance contrast spectra of $SnSe_2$ flakes of different thickness on SiO_2/Si substrate are also measured at 4K. The dip in the reflectance contrast is found to change its spectral position with $SnSe_2$ thickness as observed at room temperature. Even at this low temperature, the dip is still spectrally broad and does not show any sharp excitonic feature. This helps to confirm that transition dipole in $SnSe_2$ is governed by free electron-hole pairs as the screening offered by the large carrier concentration suppresses strongly bound exciton state in $SnSe_2$.

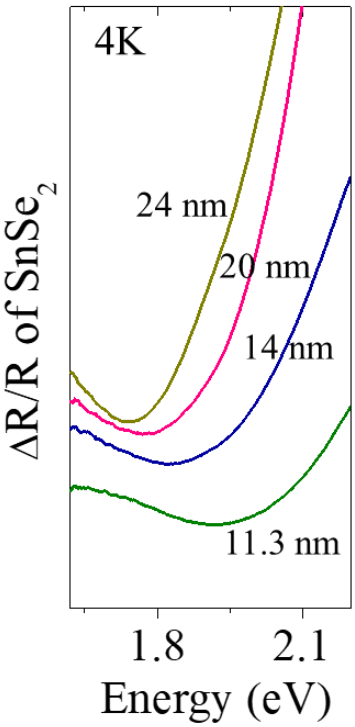

Figure S4: Reflectance contrast spectra of isolated $SnSe_2$ flakes on SiO_2/Si substrate at 4 K. Corresponding thickness of $SnSe_2$ is indicated at each spectrum.

Photoluminescence spectroscopy across 2L-MoS_2/$SnSe_2$

Unlike 1L-MoS_2, 2L-MoS_2 does not exhibit any PL enhancement on the junction with $SnSe_2$. Figure S5a shows the quenched PL spectra of 2L-MoS_2/$SnSe_2$ with 633 nm at different temperatures. From Figure S5b we can see that there is decrease in PL quenching with increase in temperature like that of 1L-MoS_2/$SnSe_2$. The absence of PL enhancement in the case of 2L-MoS_2/$SnSe_2$ can be correlated with the competition between the rate of FRET and increased non-radiative scattering in bilayer as seen from the model in the next section.

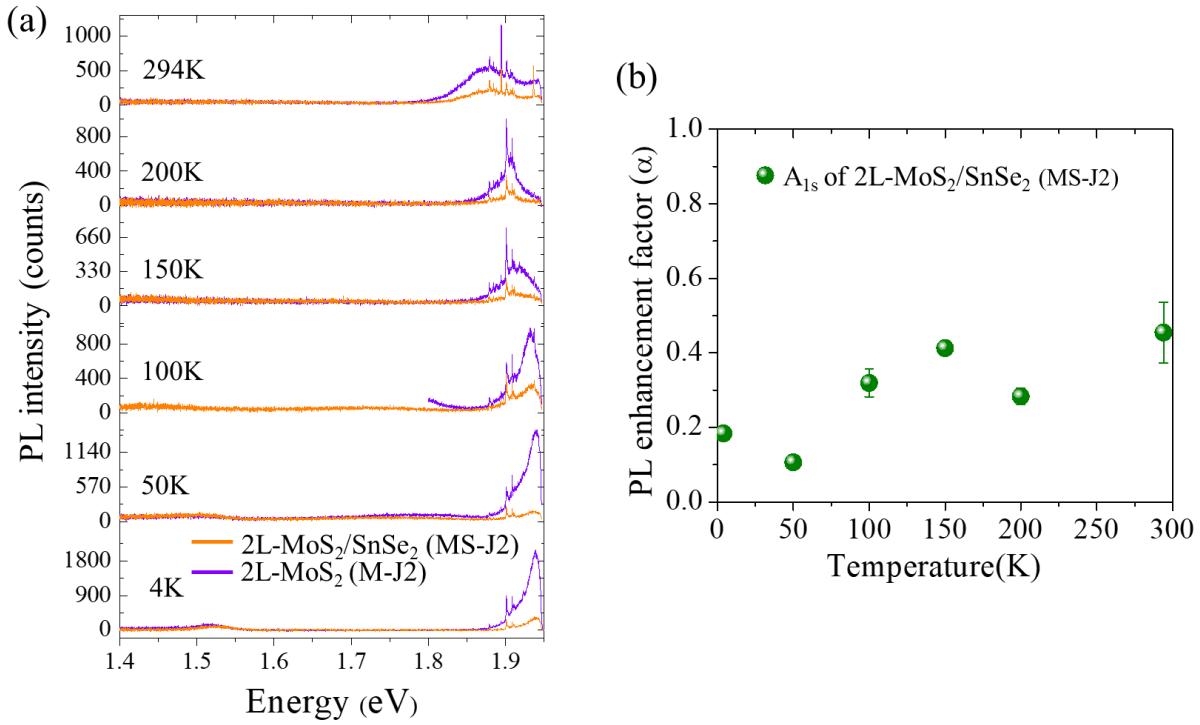

Figure S5: (a) Temperature dependent PL spectra of 2L-MoS_2 (violet) and its junction with $SnSe_2$ (orange) from sample J2 under 633 nm excitation. (b) Variation of PL enhancement factor (α) of A_{1s} exciton peak of 2L-MoS_2/$SnSe_2$ with 633 nm excitation.

Discussion on the rate of FRET and PL enhancement factor

Deriving PL enhancement factor from the rate equations:

Experimental data proves that the PL enhancement observed across different layered heterostructures is sensitive to excitation wavelength (resonant versus non-resonant), temperature, donor and acceptor materials, thickness of the donor and the acceptor, and the separation between them. To get a qualitative understanding of the effect of these parameters, we derive an expression for the PL enhancement factor from the rate equations of exciton density in the isolated 1L-MoS_2 and the 1L-MoS_2 /$SnSe_2$ junction.

Rate equations for Monolayer MoS_2 on SiO_2 with resonant excitation:

633 nm excitation near resonantly excites the exciton states of 1L-MoS_2. Let G_{ex}^{M} be the generation rate of A_{1s} excitons with 633 nm in 1L-MoS_2 on SiO_2. These excitons can either recombine radiatively at a rate Γ_r to give out photoluminescence or decay non-radiatively at a rate Γ_{nr}^{M}. The non-radiative decay (Γ_{nr}) comprises of scattering to the defect states at lower energies and scattering to the energy states outside the light cone as schematically shown in Figure 4b. The rate equation for the exciton density (N_{ex}^{M}) density in isolated 1L-MoS_2 on SiO_2 can be written as the following.

$$\frac{dN_{ex}^{M}}{dt} = G_{ex}^{M} - (\Gamma_r + \Gamma_{nr}^{M})N_{ex}^{M} \quad (1)$$

The steady state photoluminescence signal from a given excitation will be proportional to the fraction of steady state exciton density, $N_{ex}^{M} = \frac{G_{ex}^{M}}{(\Gamma_r+\Gamma_{nr}^{M})}$ decaying radiatively. So, the PL intensity from 1L-MoS_2 on SiO_2 is given to be

$$I_M \propto \frac{G_{ex}^{M}\Gamma_r}{(\Gamma_r + \Gamma_{nr}^{M})} \quad (2)$$

Rate equations for Monolayer MoS_2 on $SnSe_2$ with resonant excitation:

As shown in the schematic, 633 nm near resonantly excites multi-layer $SnSe_2$ along with 1L-MoS_2. This excitation creates free electron hole pairs in $SnSe_2$ at its direct bandgap at a rate G_{e-h}^{S} (not excitons because of screening of carriers in the degenerately doped $SnSe_2$). These free electron

hole pairs are coupled to the A_{1s} exciton states via FRET at a rate of Γ_{ET}^{S-M} or they can be scattered from the energy states in $SnSe_2$ (resonant to A_{1s} of MoS_2) to other non-resonant energy states predominantly to the states at the indirect band gap at a rate Γ_s. Excitons in 1L-MoS_2 either excited with 633 nm on the junction or created with FRET from $SnSe_2$ will also be coupled to the states in $SnSe_2$ through the process of FRET and thus they can decay to $SnSe_2$ by this dipole-dipole coupling at a rate denoted by Γ_{ET}^{M-S}. Electrons and holes from exciton state in MoS_2 can also dissociate to lower energy states in conduction and valence bands of $SnSe_2$ which causes decay of excitons through charge transfer at a rate of Γ_{CT}^{M-S}. The non-radiative decay rate of excitons on the junction Γ_{nr}^{jun} can be different from Γ_{nr}^{M} as seen from the change of broadening of PL peaks on the junction. However, the radiative decay rate Γ_r is assumed to similar in 1L-MoS2 and the junction. Generation rate of free e-h pairs in $SnSe_2$ and excitons in MoS_2 on the junction are assumed to be similar to the rates in individual layers. From the above discussion, the rate equations for exciton density in 1L-MoS_2 on the junction $(N_{ex}^{M,jun})$ and free e-h pair density in $SnSe_2$ $(N_{e-h}^{S,jun})$ can be expressed as

$$\frac{dN_{ex}^{M,jun}}{dt} = G_{ex}^{M} - \left(\Gamma_r + \Gamma_{nr}^{M,jun} + \Gamma_{CT}^{M-S} + \Gamma_{ET}^{M-S}\right)N_{ex}^{M,jun} + \Gamma_{ET}^{S-M}N_{e-h}^{S,jun} \quad (3)$$

$$\frac{dN_{e-h}^{S,jun}}{dt} = G_{e-h}^{S} - \left(\Gamma_s + \Gamma_{ET}^{S-M}\right)N_{e-h}^{S,jun} + \left(\Gamma_{CT}^{M-S} + \Gamma_{ET}^{M-S}\right)N_{ex}^{M,jun} \quad (4)$$

Since an order of enhancement is seen in the PL intensity of 1L-MoS_2 on the junction, the contribution of G_{ex}^{M} in (3) can be neglected. From (3) and (4), $I_{M,jun}$ can be obtained from $N_{ex}^{M,jun}$ as

$$N_{ex}^{M,jun} = \frac{G_{e-h}^{S}\Gamma_{ET}^{S-M}}{\Gamma_s\left(\Gamma_r + \Gamma_{nr}^{M,jun} + \Gamma_{CT}^{M-S} + \Gamma_{ET}^{M-S}\right) + \Gamma_{ET}^{S-M}\left(\Gamma_r + \Gamma_{nr}^{M,jun}\right)} \quad (5)$$

$$I_{M,jun} \propto N_{ex}^{M,jun}\Gamma_r \quad (6)$$

The PL enhancement factor, α is the ratio of steady state PL intensity of A_{1s} peak from 1L-MoS_2/$SnSe_2$ $(I_{M,jun})$ to that of 1L-MoS_2 on SiO_2 (I_M).

$$\alpha = \frac{\left(\frac{G_{e-h}^{S}}{G_{ex}^{M}}\right)\Gamma_{ET}^{S-M}}{\Gamma_s\left(\frac{\Gamma_r + \Gamma_{nr}^{M,jun}}{\Gamma_r + \Gamma_{nr}^{M}} + \frac{\Gamma_{CT}^{M-S} + \Gamma_{ET}^{M-S}}{\Gamma_r + \Gamma_{nr}^{M}}\right) + \Gamma_{ET}^{S-M}\left(\frac{\Gamma_r + \Gamma_{nr}^{M,jun}}{\Gamma_r + \Gamma_{nr}^{M}}\right)} \quad (7)$$

To get a preliminary insight into the role of different rate parameters on α, it is reasonable to ignore the difference between $\Gamma_{nr}^{M,jun}$ and Γ_{nr}^{M}. α can now be expressed as

$$\alpha = \left(\frac{G_{e-h}^{S}}{G_{ex}^{M}}\right)\frac{\gamma}{\gamma + \beta} \quad (8)$$

where $\gamma = \frac{\Gamma_{ET}^{S-M}}{\Gamma_s}$ and $\beta = 1 + \left(\frac{\Gamma_{CT}^{M-S} + \Gamma_{ET}^{M-S}}{\Gamma_r + \Gamma_{nr}^{M}}\right)$.

Temperature dependence of the rate of FRET:

As seen from eq-(7), variation of α with temperature can be related to the temperature dependent rate of different processes on illumination. Γ_{CT} and Γ_r are very weakly dependent on the temperature while Γ_{ET} and Γ_{nr} that vary with temperature can play a role in determining the value of α. We adopt the energy transfer model by Lyo[2] based on dipole-dipole coupling across quantum wells to understand the temperature dependence of α in our case. This model deals with the energy transfer from an exciton to a free e-h pair which predicts its rate as

$$\Gamma_{ET} = \Gamma_{ET}^{0}(\xi_T)\, g\left(\frac{d}{\xi_T}\right) \quad (9)$$

where d is the physical separation between the donor and the acceptor layers and ξ_T is a temperature dependent parameter, $\xi_T = \sqrt{\frac{\hbar^2}{2Mk_BT}}$ where k_B is the Boltzmann constant and M is the total mass of exciton ($M=m_e+m_h$) which is assumed to be same for both the layers.

$\Gamma_{ET}^{0}(\xi_T) = \frac{32\pi\mu}{\hbar^3}\left(\frac{q^2 D_1 D_2}{\kappa a_B \xi_T}\right)^2$ which depends the system of donor and acceptor with μ as reduced exciton mass, a_B is the exciton bohr radius, κ is the average dielectric constant, D_1 and D_2 are the dipole moments of the donor and the acceptor. g(t) is expressed as

$$g(t) = \int_0^\infty x^3 e^{-x^2} e^{-2tx} S(tx)^2\, dx \quad (10)$$

with $s(t) = \frac{\sin\left(\frac{tb_1}{2d}\right)}{\frac{tb_1}{2d}} \frac{\sin\left(\frac{tb_2}{2d}\right)}{\frac{tb_2}{2d}}$, where b_1 and b_2 are the thickness of the donor and the acceptor respectively. To project the variation of FRET in our case, we assume that rate of energy transfer is of similar magnitude in both the directions across MoS_2 and $SnSe_2$ and therefore (9) can be applicable to calculate both Γ_{ET}^{S-M} and Γ_{ET}^{M-S}. Assuming b_1=10 nm ($SnSe_2$), b_2=1 nm (MoS_2), d=1 nm and M ~ m_o in $SnSe_2$,[3] we obtain the temperature dependence of Γ_{ET} as shown in Figure S6a. Using the above variation of Γ_{ET} and (8) with assumption of parameters $\Gamma_{CT} = 10^{12}$ s^{-1}, $\Gamma_{nr} + \Gamma_r = 0.5x10^{12}$ s^{-1}, $\Gamma_s = 10^{13}$ s^{-1} and $\left(\frac{G_{e-h}^{S}}{G_{ex}^{M}}\right)$=10, an evaluation of α is done at multiple temperature which matches with the trend of experimental data as in Figure S6b.

(8) also explains the absence of enhancement for trion in 1L-MoS_2 from the interplay between FRET and radiative recombination. As Figure S6c shows the variation of α with Γ_{ET} and Γ_r keeping all other rate parameters fixed. α > 1 for those cases where β < γ which indicates that Γ_r should be fast enough to yield luminescence of FRET coupled dipoles in the acceptor. It has been shown experimentally that trion has a longer life time than exciton which makes Γ_r of exciton higher than that of trion.[4] This increased lifetime of trion accelerates their loss from MoS_2 to $SnSe_2$ and hinders the luminescence of trions from energy transferred dipoles.

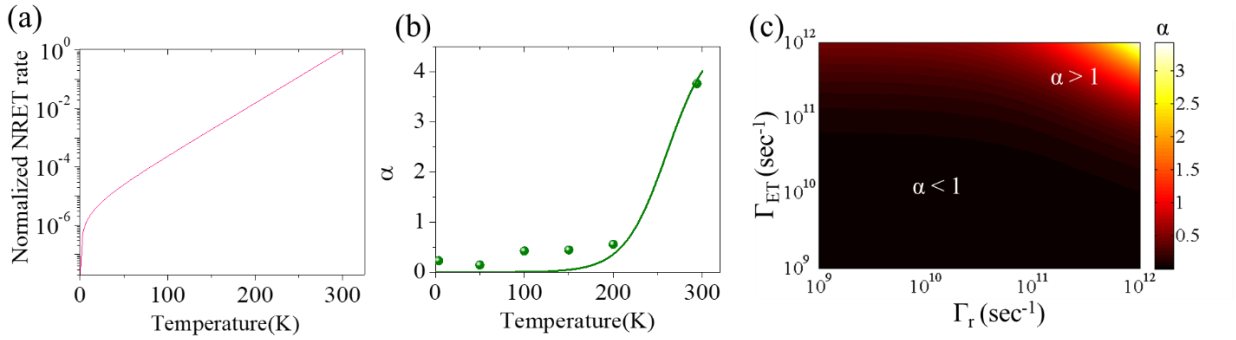

Figure S6: (a) Variation of the rate of FRET with temperature calculated from theoretical model. The y-axis is normalized with respect to the FRET rate at 300K. (b) Experimental (symbol) and model predicted (line) values of enhancement factor (α) calculated at different temperatures with 532 nm excitation. (c) Color plot of variation of enhancement factor (α) with change in the rate of FRET and the rate of radiative recombination. The enhancement (α > 1) and quenching (α < 1) regions are indicated.

References:

(1) Chakraborty, B.; Matte, H. S. S. R.; Sood, A. K.; Rao, C. N. R. Layer-Dependent Resonant Raman Scattering of a Few Layer MoS_2. *J. Raman Spectrosc.* **2013**, *44*, 92–96.

(2) Lyo, S. K. Energy Transfer of Excitons between Quantum Wells Separated by a Wide Barrier. *Phys. Rev. B - Condens. Matter Mater. Phys.* **2000**, *62*, 13641–13656.

(3) Gonzalez, J. M.; Oleynik, I. I. Layer-Dependent Properties of SnS2 and SnSe2 Two-Dimensional Materials. *Phys. Rev. B* **2016**, *94*, 125443.

(4) Wang, H.; Zhang, C.; Chan, W.; Manolatou, C.; Tiwari, S.; Rana, F. Radiative Lifetimes of Excitons and Trions in Monolayers of the Metal Dichalcogenide MoS2. *Phys. Rev. B* **2016**, *93*, 045407.